



Fam20C overexpression in odontoblasts regulates dentin formation and odontoblast differentiation

Kohei Naniwa^{1,2} · Katsutoshi Hirose¹ · Yu Usami¹ · Kenji Hata³ · Rikita Araki⁴ · Narikazu Uzawa² · Toshihisa Komori⁵ · Satoru Toyosawa¹

Received: 14 October 2022 / Accepted: 27 April 2023 / Published online: 26 June 2023
© The Author(s), under exclusive licence to Springer Nature B.V. 2023

Abstract

FAM20C phosphorylates secretory proteins at S-x-E/pS motifs, and previous studies of Fam20C-deficient mice revealed that FAM20C played essential roles in bone and tooth formation. Inactivation of FAM20C in mice led to hypophosphatemia that masks direct effect of FAM20C in these tissues, and consequently the direct role of FAM20C remains unknown. Our previous study reported that osteoblast/odontoblast-specific *Fam20C* transgenic (Fam20C-Tg) mice had normal serum phosphate levels and that osteoblastic FAM20C-mediated phosphorylation regulated bone formation and resorption. Here, we investigated the direct role of FAM20C in dentin using Fam20C-Tg mice. The tooth of Fam20C-Tg mice contained numerous highly phosphorylated proteins, including SIBLINGs, compared to that of wild-type mice. In Fam20C-Tg mice, coronal dentin volume decreased and mineral density unchanged at early age, while the volume unchanged and the mineral density elevated at maturity. In these mice, radicular dentin volume and mineral density decreased at all ages, and histologically, the radicular dentin had wider predentin and abnormal apical-side dentin with embedded cells and argyrophilic canaliculi. Immunohistochemical analyses revealed that abnormal apical-side dentin had bone and dentin matrix properties accompanied with osteoblast-lineage cells. Further, in Fam20C-Tg mice, DSPP content which is important for dentin formation, was reduced in dentin, especially radicular dentin, which might lead to defects mainly in radicular dentin. Renal subcapsular transplantations of tooth germ revealed that newly formed radicular dentin replicated apical abnormal dentin of Fam20C-Tg mice, corroborating that FAM20C overexpression indeed caused the abnormal dentin. Our findings indicate that odontoblastic FAM20C-mediated phosphorylation in the tooth regulates dentin formation and odontoblast differentiation.

Keywords FAM20C · Phosphorylation · Dentin · DSPP · Mineralization · Odontoblast differentiation

Introduction

Family with sequence similarity 20, member C (FAM20C) is a Golgi-enriched kinase that can phosphorylate multiple proteins via a S-x-E/pS motif in the secretory pathway (Tagliabracci et al. 2012, 2015). *Fam20C* is highly expressed in osteoblasts/osteocytes, ameloblasts, and odontoblasts (Hao et al. 2007; Wang et al. 2010; Oya et al. 2017). In humans, loss-of-function mutations result in lethal/non-lethal Raine syndrome, characterized by skeletal and dental abnormalities as well as hypophosphatemia and increased serum fibroblast growth factor 23 (FGF23) levels (Raine et al. 1989; Simpson et al. 2007; Faundes et al. 2014; Acevedo et al.

2015). Global Fam20C-deficient mice (*Sox2-Cre;Fam20C^{fl/fl}*) exhibit hypophosphatemic rickets/osteomalacia and small abnormal teeth with severe enamel defects, thin dentin, enlarged pulp chambers, and undeveloped roots (Vogel et al. 2012; Wang et al. 2012; Liu et al. 2020). Mineralized, tissue-specific Fam20C-deficient mice (*Colla1-Cre;Fam20C^{fl/fl}*) show milder phenotypes of hypophosphatemic rickets/osteomalacia and tooth abnormalities (Liu et al. 2014, 2017). Craniofacial mesenchymal cell-specific Fam20C-deficient mice (*Wnt1-Cre;Fam20C^{fl/fl}*, *Osr2-Cre;Fam20C^{fl/fl}*) present with remarkable dentin and alveolar bone defects with mild hypophosphatemia (Wang et al. 2015). Epithelial cell-specific Fam20C-deficient mice (*K14-Cre;Fam20C^{fl/fl}*) have severe enamel defects with no hypophosphatemia (Wang et al. 2013). Fam20C-induced hypophosphatemia is an important cause of these severe hard-tissue defects. However, considering that these defects do not completely

Kohei Naniwa and Katsutoshi Hirose are contributed equally.

Extended author information available on the last page of the article

resolve after treatment with a high phosphate diet (Zhang et al. 2019, 2021), FAM20C is likely to play a critical direct role in bone and dental tissues.

FAM20C phosphorylates Small-Integrin-Binding ligand, N-linked Glycoproteins (SIBLINGs), which are the major non-collagenous proteins in bone and dentin (Ishikawa et al. 2012; Tagliabracci et al. 2012, 2013). Phosphorylation of SIBLINGs makes them highly negatively charged, which may assist in the recruitment of calcium ions and the nucleation and growth of hydroxyapatite crystals (Qin et al. 2004; George and Veis 2008; Deshpande et al. 2011). To elucidate the role of FAM20C in bone and dental tissues, most previous studies have used Fam20C-deficient mice; however, these mice develop systemic hypophosphatemia that masks the direct effect of FAM20C in mineralized tissues. On the other hand, our previous study reported that osteoblast/odontoblast-specific *Fam20C* transgenic (Fam20C-Tg) mice exhibited no alteration in serum phosphate levels (Hirose et al. 2020). FAM20C phosphorylates Ser¹⁸⁰ in active iFGF23 (intact full-length FGF23), and this phosphorylation event induces cleavage of iFGF23 into two inactive FGF23 fragments (Acevedo et al. 2015). In fact, the serum level of cleaved inactive FGF23 was significantly higher in Fam20C-Tg than in WT mice in previous paper (Hirose et al. 2020). However, there is no significant difference of active iFGF23 between the two and hence Fam20C-Tg mice exhibited no alteration in serum phosphate levels. In this way, our previous paper reported that osteoblastic FAM20C-mediated phosphorylation directly regulated bone formation and resorption and bone material quality (Hirose et al. 2020). As a results, cortical bone in Fam20C-Tg mice had the increased volume and mineralization with elevated number of vascular canals and osteocytes while trabecular bone had decreased volume and unchanged mineralization.

Bone and tooth dentin are both collagen-based mineralized tissues, and dentin, unlike bone, contains tissue-specific dentin sialophosphoprotein (DSPP), which plays important roles in dentin formation (Qin et al. 2004; Prasad et al. 2010). The importance of DSPP in dentin formation is supported by its association with mutations of the *Dspp* gene in human dentinogenesis imperfecta (Zhang et al. 2001) and defective dentin mineralization in DSPP-deficient mice (Sreenath et al. 2003). DSPP is proteolytically processed to dentin sialoprotein (DSP, the NH₂-terminal fragment) and dentin phosphoprotein (DPP, the COOH-terminal fragment) (Feng et al. 1998). DSPP is highly phosphorylated; in particular, DPP contains repeating S-S-D sequences and a high proportion of phosphoserine, which comprises more than 40% of the total amino acids (Butler et al. 1983; Qin et al. 2004). The biochemical characteristics of phosphoserine are important in dentin formation (Zhang et al. 2018). However, the motif surrounding phosphoserines in DPP rarely conforms to the S-x-E/pS FAM20C consensus motif. Even if

there is few, phosphorylation by additional protein kinases may prime DPP by creating a S-X-pS FAM20C recognition motif. Phosphorylation of DSPP may occur in this hierarchal manner (Roach 1991). Otherwise, FAM20C may phosphorylate the S-S-D motifs of DPP since FAM20C has broader substrate specificity that previously appreciated (Tagliabracci et al. 2015). Furthermore, in vitro loss-of-function experiments indicated that FAM20C accelerated the differentiation of mesenchymal stem cells into odontoblasts and promoted mineralized nodule formation (Li et al. 2018; Liu et al. 2018b). Thus, it is possible that FAM20C phosphorylates DSPP and plays a vital role in dentin formation.

In this study, we investigated the role of odontoblastic FAM20C-mediated phosphorylation in dentin formation in Fam20C-Tg mice.

Materials and methods

Fam20C transgenic mice (Fam20c-Tg)

Fam20C-Tg mice on a C57BL/6 genetic background were generated as previously described (Hirose et al. 2020). Exogenous mouse *Fam20C* was driven by a 2.3-kb pro- α 1(I) collagen promoter. All experiments were performed using only male mice between 1 and 24 weeks of age. C57BL/6 mice and C.B-17/*Icr-scid/scid*Jcl (SCID) mice were purchased from CLEA Japan, Inc. (Osaka, Japan). All animal experiments were reviewed and approved by the Intramural Animal Use and Care Committee of Osaka University Graduate School of Dentistry (Permit Number R-01-006-0).

Histological analyses

For histological analyses, mice at 1, 4, 8, or 12 weeks of age were euthanized and fixed in 4% paraformaldehyde (PFA) in 0.1 M sodium phosphate buffer (pH 7.4) (PBS). Jaws containing teeth were excised and further fixed by immersion in the same fixative. The samples then were decalcified in 10% EDTA solution (pH 7.4) and embedded in paraffin. Section (4- μ m thickness) were used for hematoxylin and eosin (HE), silver impregnation, and immunohistochemical staining.

Immunohistochemical analyses with the LSAB method (DakoCytomation, Glostrup, Denmark) was performed using anti-FAM20C antibody (1:200 dilution, Abcam, Cambridge, MA, USA), anti-DSP antibody (1:1000 dilution, Sigma-Aldrich, St. Louis, MO, USA), anti-DPP antibody (1:5000 dilution, Kerfast, Boston, MA, USA), anti-dentin matrix protein 1 (DMP1) antibody (Toyosawa et al. 2001), anti-osteopontin (OPN) antibody (1:1000 dilution, Immuno-Biological Laboratories Co., Ltd., Gunma, Japan), anti-runt-related transcription factor 2 (Runx2) antibody (1:1000

dilution, Medical Biological Laboratories Co., Ltd., Nagoya, Japan), and anti-phosphoserine antibody (1:1000 dilution, Sigma-Aldrich), anti-NESTIN (1:1000 dilution, Merck Millipore, Darmstadt, Germany) and anti-bone morphogenetic protein 2 (BMP2) antibody (1:5000 dilution, Elabscience, TX, USA). After the sections were washed, they were incubated with biotinylated secondary antibodies, rinsed, and incubated with streptavidin–horseradish peroxidase (HRP; DakoCytomation). To visualize the immunoreaction sites, the sections were incubated with 3-amino-9-ethylcarbazole (DakoCytomation) and counterstained with hematoxylin or methyl green. Silver impregnation staining was performed as previously described (Kusuzaki et al. 2000). These specimens were used for histological and quantitative analyses. Quantification of the phosphoserine immunoreactivity was performed using NIH ImageJ software (<https://imagej.nih.gov/ij/>).

Microphotographs were obtained with an Eclipse E600 microscope (Nikon, Tokyo, Japan) equipped with a digital camera. The areas of radicular dentin and pre-dentin below the cement–enamel junction of the mesial root in the upper first molars were measured by ImageJ software. Double fluorochrome labeling was performed to analyze mineral deposition in the dentin. Briefly, 4-week-old mice were subcutaneously injected with alizarin (red fluorescence) (Sigma-Aldrich) at a dose of 0.02 mg/g body weight 5 days before termination, and tetracycline hydrochloride (green–yellow fluorescence) (Sigma-Aldrich) at a dose of 0.02 mg/g body weight 2 days before termination. After sacrifice, jaws containing teeth were immediately fixed in 70% ethanol, dehydrated, embedded in OCT compound, and frozen. Undecalcified frozen section (10- μ m thickness) of the mesial root of the first molars were viewed using ZEISS Axio Vert.A1 (Carl Zeiss). Alizarin and tetracycline depositions in the root dentin of WT and Fam20C-Tg mice were traced and photographed. The fluorescence distance between the two types of deposition were measured using ImageJ, and the mineral appositional rate of root dentin was determined.

Phosphoproteomic analysis

Phosphoproteomic analysis was performed by Medical ProteoScope (Yokohama, Japan) using modifications of previously described methods (Nagata et al. 2015). Proteins were extracted from the upper first molars of 4-week-old mice using lysis buffer (4 M guanidine–HCl, 0.5 M EDTA, pH 7.4) for 72 h at 4 °C. After that, lysis buffer was replaced with new lysis buffer (20 mM HEPES–NaOH, pH 8.0, 9 M urea). The proteins were digested with bovine trypsin for 16 h at room temperature, and then all peptides were pooled and lyophilized. To concentrate phosphopeptides, the peptide mixture was loaded onto a titanium dioxide (TiO₂) tip column with the Titan sphere Phos-TiO Kit (GL Sciences,

Inc., Tokyo, Japan). LC–MS/MS analysis, peptide identification, and quantification were performed using the phosphopeptide samples according to previously described methods (Nagata et al. 2015).

Gene ontology (GO) enrichment analysis

To elucidate the biological function of the identified proteins, GO enrichment analysis was performed using DAVID Bioinformatics Resources 6.8 (<https://david.ncifcrf.gov/>) (Nagata et al. 2015).

Micro-computed tomography (μ CT) analysis

Jaws containing teeth were dissected from euthanized mice at 2, 4, 8, 12, or 24 weeks of age. μ CT analysis was performed on a μ CT system [R_mCT (Rigaku Corporation, Tokyo, Japan)]. High-resolution 2D representations of the upper first molar at 4 weeks of age were acquired using SKYSCAN 1272 (BRUKER, Yokohama, Japan).

RNA extraction and quantitative real-time PCR analysis

Real-time PCR was performed using RNA isolated from upper first molars at 4 weeks of age. Total RNA was extracted using TRIzol (Thermo Fisher Scientific, Carlsbad, CA, USA) and the RNeasy Mini Kit (Qiagen, Hilden, Germany). Primer sequences are shown in Table 1. Values were normalized against the corresponding levels of *GAPDH* mRNA.

Western blotting

Western blotting was performed using proteins isolated from upper first molars at 4 weeks of age. Protein was extracted using lysis buffer (20 mM HEPES–NaOH, pH 8.0, 9 M urea, 0.5 M EDTA, Phosphatase Inhibitor Cocktail solutions 1 and 2, Sigma-Aldrich) (Nagata et al. 2015). After quantification of protein concentration, lysates containing equal amounts of total proteins were subjected to SDS-PAGE (Wako). To visualize proteins, gels were stained with Coomassie brilliant blue (CBB). The proteins were transferred to polyvinylidene membranes (Global Life Science Technologies Japan, Tokyo, Japan), which were incubated with anti-DPP antibody (1:1000 dilution, Santa Cruz Biotechnology, Dallas, TX, USA) and then incubated with HRP-conjugated secondary antibody (Santa Cruz Biotechnology). Blots were visualized with the Enhanced Chemiluminescence Kit (Amersham Biosciences).

Table 1 Primers used for real-time PCR analyses

Gene symbol	Forward primer	Reverse primer
<i>Fam20C</i>	TGAAGATGATACTGGTGCGCAGGT	CAACAGCAATGTGCAAAGCGCAAG
<i>Runx2</i>	CTTCGTCAGCATCCTATCAGTTC	TCAGCGTCAACACCATCATTC
<i>Osx</i>	CTACCCAGCTCCCTTCTCAA	CTTGTACCACGAGCCATAGG
<i>Col1a1</i>	CCTGGAATGAAGGGACACCG	CCATCGTTACC CGGAGCACC
<i>Alp</i>	CGCACGCGATGCAACACCAC	TGCCACGGACTTCCCAGCA
<i>Opn</i>	GCAGAATCTCCTTGCGCCAC	CGAGTCCACAGAATCCTCGC
<i>Dmp1</i>	CGCATCCCAATATGAAGACTG	GCTTGACTTTCTTCTGATGACTCA
<i>Dspp</i>	ATTCCGGTCCCCAGTTAGTA	CTGTTGCTAGTGGTGCTGTT
<i>Nestin</i>	CCCTGAAGTCGAGGAGCTG	CTGCTGCACCTCTAAGCGA
<i>Bmp2</i>	GGAAGACGTCTCAGCGAAT	ACGGTCTTTCGTGATGGAA
<i>GAPDH</i>	GGTGTGAACCACGAGAAA	AGTCGCAGGAGACAA

Fam20C family with sequence similarity 20, member C, *Runx2* runt-related transcription factor 2, *Osx* osterix, *Col1a1* type1 collagen α 1, *Alp* alkaline phosphatase, *Opn* osteopontin, *Dmp1* dentin matrix protein 1, *Dspp* dentin sialophosphoprotein, *Bmp2* bone morphogenetic protein 2, *GAPDH* glyceraldehyde 3-phosphate dehydrogenase

Tooth extraction experiment

To eliminate occlusal force on the apical root of the upper left first and second molars, the lower left first and second molars in WT and Fam20C-Tg mice at 2 weeks of age were extracted under combination anesthesia. Six weeks after tooth extraction, mice were euthanized and immediately fixed in PFA in 0.1 M PBS. The upper jaws that contained teeth were resected and these samples were subjected to μ CT and histological analyses. Age-matched WT and Fam20C-Tg mice with no treatment were used as controls.

Renal subcapsular transplantation

The tooth germs (before root formation) from the upper first molars were isolated from 6-day-old WT and Fam20C-Tg mice. Tooth germs were prepared for transplantation under the renal subcapsule of SCID mice. The explants were harvested after 30 days, fixed in PFA in 0.1 M PBS, and then processed for paraffin embedding. Serial sections were used for HE, silver impregnation, and immunohistochemical staining as described above.

Statistical analysis

All data are presented as the mean standard error (SE). Comparisons of two groups were evaluated using Student's t-test. A p -value < 0.05 was set to be statistically significant.

Results

Validation of Fam20C overexpression in dentin of Fam20C-Tg mice

At 4 weeks of age, the level of *Fam20C* mRNA expression, including endogenous and exogenous mouse *Fam20C* mRNA, was approximately 30-fold higher in Fam20C-Tg mice than in WT mice (Fig. 1a). At 1 and 4 weeks of age, FAM20C immunoreactivity in odontoblasts and osteoblasts was stronger in Fam20C-Tg mice than in WT mice (Fig. 1b–e). The immunoreactive intensity in coronal odontoblasts was attenuated in both genotypes at 4 weeks of age when compared to 1 week of age (solid black frames, enlarged in Fig. 1b–e). At 4 weeks of age, the immunoreactive intensity in coronal odontoblasts appeared to be lower than that in radicular dentin in both genotypes (Fig. 1d, e). Immunoreaction was also seen in the dentin matrix in Fam20C-Tg mice (Fig. 1c, e). In the upper incisor, FAM20C immunoreaction in odontoblasts on the labial and lingual sides was stronger in Fam20C-Tg mice than in WT mice at 4 weeks (Fig. 1a, b in Supplementary Material 1).

Phosphorylation state of tooth proteins in Fam20C-Tg mice

The phosphorylated peptides in tooth proteins of Fam20C-Tg mice were analyzed by LC–MS/MS. Of the 1685 peptides identified through the database search, 1545 (91.7%) were phosphorylated (Supplementary Material 2). The

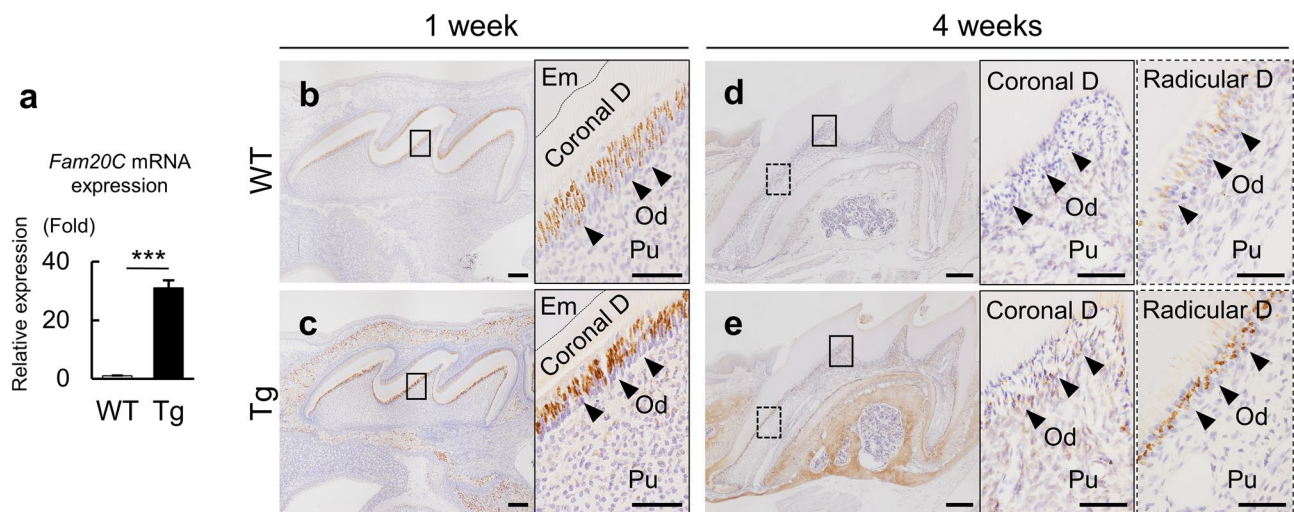


Fig. 1 Validation of *Fam20C* overexpression in dentin. **a** Real-time PCR analysis. The expression level of *Fam20C* mRNA, including both exogenous and endogenous copies, was evaluated using mRNA extracted from upper first molars at 4 weeks of age ($n=6$ in each group). Values in WT mice were defined as 1, and relative levels are shown. **b–e** Representative images of FAM20C-immunostaining in upper first molars at 1 week (**b, c**) and 4 weeks (**d, e**) of age in WT (**b, d**) and Fam20C-Tg mice (**c, e**). Transgene expression was detected in odontoblasts (arrowheads) and osteoblasts. At 1 and 4 weeks of age, FAM20C-immunoreactivity in odontoblasts and osteo-

blasts was stronger in Fam20C-Tg mice (**c, e**) than in WT mice (**b, d**). The FAM20C-immunoreactivity in coronal odontoblasts of both genotypes at 4 weeks of age (solid frames in **d, e**), was attenuated compared to 1 week of age (solid frames in **b, c**), and appeared to be lower than that in radicular dentin (dotted frames in **d, e**). Solid frames indicate higher magnification of coronal dentin and dotted frames indicate higher magnification of radicular dentin. *Versus WT mice; *** $p < 0.001$. WT WT mice, Tg Fam20C-Tg mice, Em enamel, D dentin, Od odontoblast, Pu pulp. Scale bars 200 μm in **b–e** and 50 μm in solid and dotted frames in **b–e**

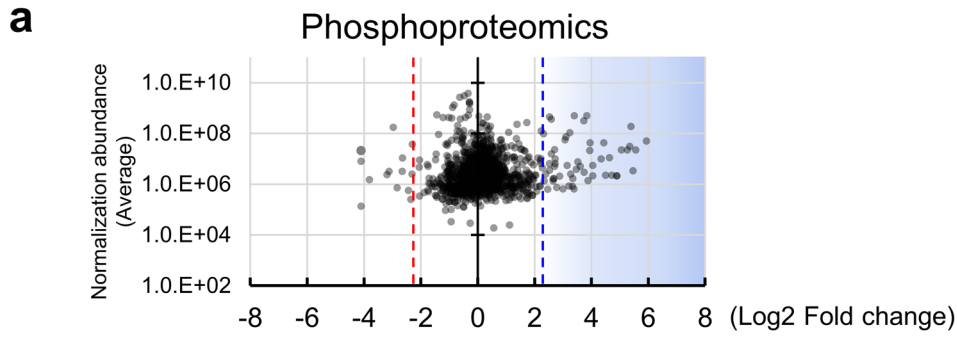
phosphorylated peptides were quantitatively compared between WT and Fam20C-Tg samples, as shown in the scatter plot in Fig. 2a. More than five times more phosphorylated peptides were detected in Fam20C-Tg samples than in WT samples (data points distributed on the right side of the dotted blue line in Fig. 2a). In addition, 172 phosphorylated peptides in Fam20C-Tg samples were detected at levels 10 times higher than those in WT samples or were detected only in Fam20C-Tg samples (Supplementary Material 2). In contrast, 39 phosphorylated peptides in Fam20C-Tg samples were detected at levels more than 10 times lower than those in WT samples or were detected only in WT samples (Supplementary Material 2). Together, these findings indicated that Fam20C overexpression in odontoblasts promotes the phosphorylation of tooth proteins.

To investigate the functions of the proteins whose phosphorylation was enhanced by Fam20C-Tg overexpression, GO analysis was performed using DAVID (Supplementary Material 3). The results showed that the proteins were mainly involved in “ossification”, “biomineral tissue development”, and “osteoblast differentiation”, and in the molecular functions of “calcium ion binding” and “insulin-like growth factor binding”, and they were localized in the extracellular matrix or involved in the extracellular secretory pathway (Supplementary Material 3).

Numerous phosphorylated peptide fragments of OPN, DMP1, and DSP (the NH₂-terminal fragment of DSPP),

which are acidic phosphorylated proteins related to calcification, were also detected (Fig. 2b). The proteomic coverage for the OPN peptides was 65%. In OPN derived from Fam20C-Tg samples, 27 phosphorylation sites (S: 24 sites, T: 2 sites, Y: 1 site) were identified. Five of the S residues (S²¹³, S²³⁸, S²⁴³, S²⁹⁰, S²⁹¹) showed enhanced phosphorylation in Fam20C-Tg mice compared to WT mice (Fig. 2b, OPN blue background). The proteomic coverage for the DMP1 peptides was 42%. In DMP1 derived from Fam20C-Tg mice, 22 phosphorylation sites (S: 15 sites, T: 6 sites, Y: 1 site) were identified. Six of the S and T residues (S²³⁷, S²⁶², S²⁶⁶, S²⁶⁹, T¹⁰⁹, T²⁸⁵) were phosphorylated at a higher level in Fam20C-Tg mice than in WT mice or were phosphorylated only in Fam20C-Tg mice (Fig. 2b, DMP1 blue background). The proteomic coverage for the DSP peptides was 18%. In DSP derived from Fam20C-Tg mice, 17 phosphorylation sites (S: 16 sites, T: 1 site) were identified. Seven of the S residues (S¹⁵², S¹⁶³, S¹⁷⁰, S³⁵⁶, S³⁸⁷, S⁴²³, S⁴²⁸) were phosphorylated at a higher level in Fam20C-Tg mice than in WT mice or were phosphorylated only in Fam20C-Tg mice (Fig. 2b, DSP blue background). In this way, FAM20C can also phosphorylate broader substrates with the other motif of the S-x-E/pS.

On the other hand, in OPN, DMP1, and DSP proteins derived from WT samples, no phosphorylation sites exhibited increased phosphorylation compared to those in Fam20C-Tg mice or were phosphorylated only in WT



b

OPN
 1 mrlavicfcl fgiasslpvk vtdsgsseek lyslhpdpia twlvdpdsqk qnllapqnav
 61 sseekddfkdq etlpsnsnes hdhmdddddd ddddgdhaes edsvdsdesd eshhsdesde
 121vtvastqadt ftpivptvdv pngrgds lay glrskrsfq vsdeqypdat dedltshms
 181geskesldvi pvaqllmmps dqdnngkqsh essqldepsi ethrlehskes qesadqsdv
 241idsqasskas lehqshkfhsh hkdvlvldpk skeddrylkf rishelssss sevn

DMP1
 1 mktvillvfl wglscalpva ryhntesess eertddlags ppptnsess eesqaspegq
 61 ansdhtdsse sgeelgydrg qyrpagglisk stgtgdkdd deddsgdtdf gdednglqpe
 121egqwgppskl dsdedtsadt qssedstsqe nsaqdtpsds kdqdsedead srpeagdsaq
 181dseseerqv ggsegesshg dgsefddegm qsdpestrs drgharmssa girseeskgd
 241reptstqdsd dsqvefssr ksfrrrvse edyrgelt ds nsretqsdst edtaskeesr
 301esqedtaes qsqedspeqq dpssesseea gepssqesse sqegvteser gdnpdntsqt
 361gdqedsesse edslnfss esqsteeqad sesneslsls eesqesaqdg dsssgeqlqs
 421qsastesrsq esqseqdrrs eedsdsqds rskeensng sa sssseedir pknmeadsrk
 481livdayhnkp igdqddndcq dgy

DSP
 1 mkmkiiiyic iwatawaipv pqlvplerdi vensvavpll thpgtaaqne lsinsttss
 61 ndspdgseig eqvlsegyk rdngsesih vggkdfptqp ilvneqgnla eehndietyg
 121hdgvhargen stangirsqv givenaeae ssvhgqagqn tksggasdvsnqngdatlvqe
 181neppeasikn stnheagihg sgvatthetp qreglgsenq gtevtpsige dagldtdgs
 241psngveede dtgsgdgega eagdgreshd gtkgqqgqsh ggntdhrqqs svstedddsk
 301eqegfpnghn gdnssseengv eegdstqatq dnqklspkdt rdaeggisq seacpsgksq
 361dqgie tegpn kgnksiiitke sgklsgskds nghqgveldk rnspkqgesd kpqgtaeksa
 421ahsnlghsri gssnsndghd syefddesmq g

Anti-Phosphoserine

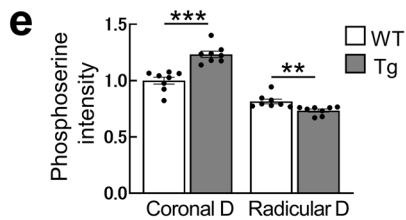
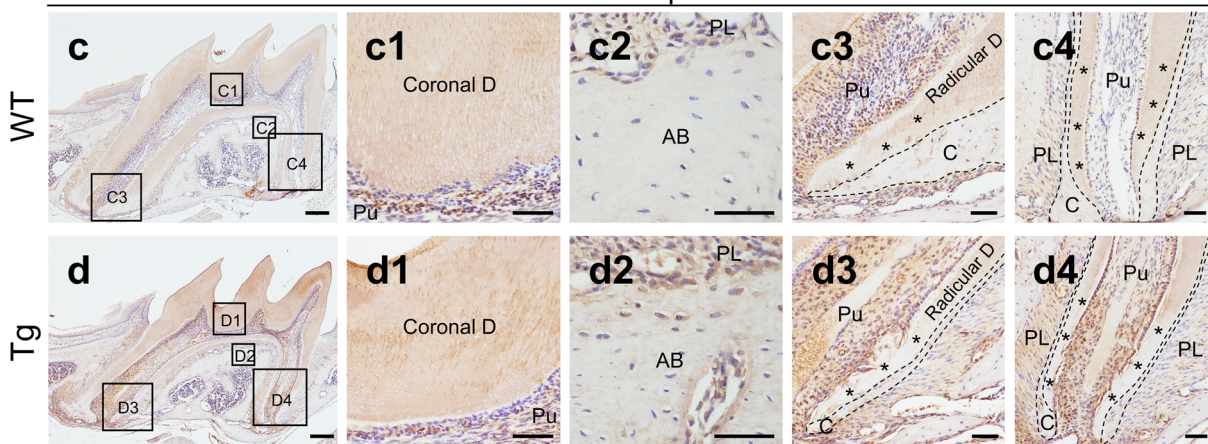


Fig. 2 Phosphorylation state of tooth proteins in Fam20C-Tg mice. **a** Scatter plot of phosphorylated peptides. Proteins were extracted from upper first molars at 4 weeks of age. Phosphorylated peptides were recovered and subjected to LC–MS/MS. The points to the right of the dotted blue line indicate phosphorylated peptides that were detected more than five times more frequently in Fam20C-Tg mice than in WT mice (blue region). The points to the left of the dotted red line indicate phosphorylated peptides that were detected more than five times less frequently in Fam20C-Tg mice than in WT mice. **b** Phosphorylation state of SIBLINGs. In the OPN, DMP1, and DSP amino acid sequences subjected to comprehensive phosphorylation analysis (underlined), the phosphorylation sites are indicated by yellow and blue backgrounds. A blue background indicates sites where the phosphorylation rate of the peptide derived from Fam20C-Tg mice was more than twice that of the same peptide derived from WT mice. For example, when the phosphorylation rate of S²¹³ in OPN was calculated as the number of phosphorylated S²¹³ residues divided by the total number of S²¹³ residues in WT and Fam20C-Tg mice, the phosphorylation rate of S²¹³ in WT mice was 6% and that in Fam20C-Tg mice was 20%. Compared with S²¹³ of OPN derived from WT mice, that of Fam20C-Tg mice showed more than a three-fold higher phosphorylation rate. **c, d** Representative images of immunohistochemical staining of phosphoserine. In upper first molars at 4 weeks of age, the immunoreactivity of phosphoserine in coronal dentin was enhanced in Fam20C-Tg mice compared with WT mice (**c, c1, d, d1**). Conversely, in the root, especially on the apical side, the immunoreactivity of phosphoserine was decreased in Fam20C-Tg mice compared to WT mice (asterisks in **c3, c4, d3, d4**). The immunoreactivity of phosphoserine in the alveolar bone was enhanced in Fam20C-Tg mice (**c2, d2**). **e** Quantification of phosphoserine immunoreactivity in the coronal and radicular dentin. The points indicate immunoreactivity values in coronal and radicular dentin of WT and Fam20C-Tg mice, based on immunoreactivity value of coronal dentin of WT mice (n = 8 in each group). *Versus WT mice; ** $p < 0.01$; *** $p < 0.001$. WT WT mice, Tg Fam20C-Tg mice, D dentin, C cementum, AB alveolar bone, Pu pulp, PL periodontal ligament. Scale bars 200 μm in **c** and **d** and 50 μm in **c1–c4, d1–d4**

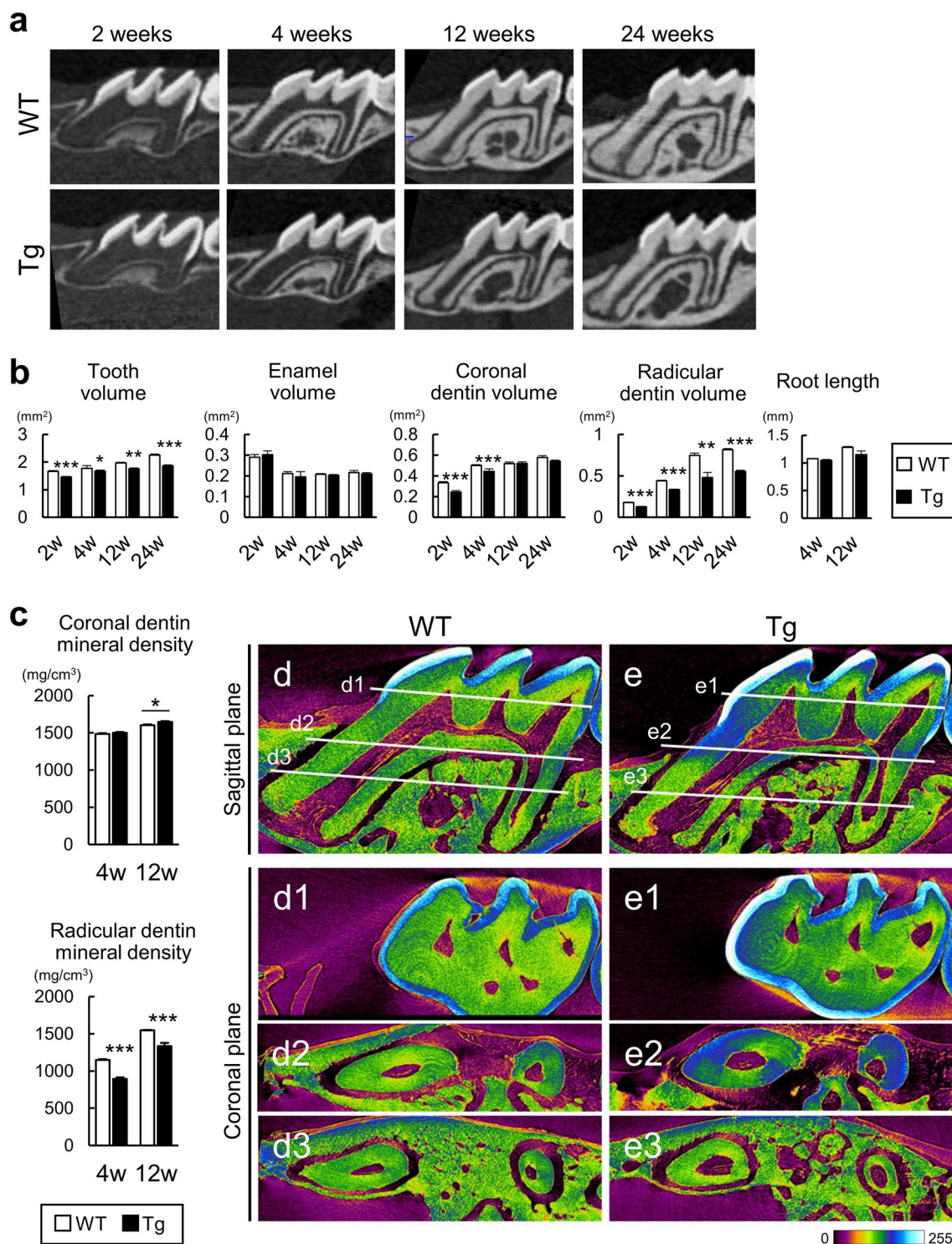
mice. DPP, the COOH-terminal fragment of DSPP, was not detected. This is because DPP is composed of repeated S-S-D (Ser-Ser-Asp) sequences and no peptide fragments suitable for LC–MS/MS detection could be obtained through trypsin hydrolysis. In enamel proteins (enamelin, ameloblastin) which have potential FAM20C phosphorylation sites (Al-Hashimi et al. 2010; Delsuc et al. 2015), we observed no difference in the degree of phosphorylation between WT and Fam20C-Tg mice (Supplementary Material 2), indicating that Fam20C overexpressed in odontoblasts is not involved in the phosphorylation of enamel proteins.

DPP, which was not detected in the phosphorylation analysis, is the most abundant non-collagen protein in dentin. As it is highly phosphorylated, almost exclusively at serine residues, the phosphorylation state in dentin can be investigated by immunohistochemical staining of phosphorylated serine (phosphoserine) (Oya et al. 2017; Hirose et al. 2020). The immunoreactivity of phosphoserine was higher in the coronal dentin of Fam20C-Tg mice than in that of WT mice, indicating that DPP phosphorylation was enhanced in Fam20C-Tg mice (Fig. 2c, c1, d, d1). In contrast, in the radicular dentin of Fam20C-Tg mice, especially on the apical side,

the immunoreactivity was attenuated when compared with that in WT, indicating reduced phosphorylation (Fig. 2c3, c4, d3, d4). Quantitative analysis showed that the immunoreactivity of phosphoserine in coronal dentin was significantly higher in Fam20C-Tg mice than WT mice, and that the immunoreactivity of phosphoserine in radicular dentin was significantly lower in Fam20C-Tg mice than WT mice (Fig. 2e). In the upper incisor, phosphoserine immunoreaction in the crown dentin analogue on the labial side was stronger in Fam20C-Tg mice than in WT mice at 4 weeks (Fig. 1c, d in Supplementary Material 1). Thus, SIBLING proteins in dentin were highly phosphorylated in Fam20C-Tg mice compared to WT mice. The immunoreactivity of phosphoserine in the alveolar bone was also enhanced upon Fam20C-Tg overexpression (Fig. 2c2, d2).

Changes of coronal and radicular dentin in Fam20C-Tg mice

A time-course analysis of the morphological changes in the upper and lower first molars by μCT revealed that root dentin formation was suppressed in Fam20C-Tg mice compared to WT mice at 2–24 weeks, and that coronal dentin seemed to be reduced in Fam20C-Tg mice compared to WT mice at 2 weeks (Fig. 3a; Fig. 2 in Supplementary Material 1). Quantitative analysis of the μCT images revealed that the total amount of dentin in the upper first molars at all ages between 2 and 24 weeks was decreased in Fam20C-Tg mice compared to WT mice, but there was no significant difference in the amount of enamel (Fig. 3b). Since decreased root dentin formation was observed on μCT images, dentin was analyzed separately for the crown and root. Although the amount of coronal dentin in Fam20C-Tg mice was significantly lower than in WT mice at 2 and 4 weeks of age, no significant difference was observed at 12 and 24 weeks of age (Fig. 3b), indicating that coronal dentin formation was reduced at early ages but recovered by maturity in Fam20C-Tg mice. The dentin mineral density in Fam20C-Tg mice did not differ from that in WT mice at 4 weeks of age, and was significantly increased at 12 weeks of age (Fig. 3c), indicating that coronal dentin mineralization was promoted in mature Fam20C-Tg mice. There was no significant difference in root length between Fam20C-Tg and WT mice (Fig. 3b), and the volume and mineral density of the radicular dentin were significantly lower in Fam20C-Tg mice than in WT mice at 4 and 12 weeks of age (Fig. 3b, c). High-resolution μCT (SKYSCAN1272) analysis of the upper first molar at 12 weeks revealed that in Fam20C-Tg mice, the dentin mineral density increased from the crown to the cervical region (Fig. 3d, e). This increase was particularly noticeable near the enamel-dentin and cement-enamel boundaries (Fig. 3d1, d2, e1, e2).



Histological analysis of the upper first molars of 4-week-old mice showed no significant difference in dentin or predentin morphology of the crown in Fam20C-Tg mice (Fig. 4a, a1, b, b1). However, the radicular dentin of Fam20C-Tg mice was narrowed, and its area was significantly reduced (Fig. 4a, b, e). In addition, the area and width of predentin and the ratio of the predentin area to the dentin

area were increased in Fam20C-Tg mice compared to WT mice (Fig. 4a2, b2, e). Silver impregnation staining revealed an argyrophilic dentin tubule structure and a canalicula-like structure extending perpendicular to the dentin tubule in the root dentin of Fam20C-Tg mice, while no argyrophilic tubule structure was found in the radicular dentin of WT mice (Fig. 4c, d, white arrows). The coronal dentin had no

Fig. 3 μ CT analysis. **a** Representative sagittal μ CT images of upper first molars at 2, 4, 12, and 24 weeks of age. Radicular dentin was decreased in Fam20C-Tg mice at all ages. Coronal dentin seemed to be decreased in Fam20C-Tg mice at 2 weeks of age. **b, c** μ CT analysis at 2, 4, 12, and 24 weeks of age. Coronal dentin volume was lower in Fam20C-Tg mice than in WT mice at 2 and 4 weeks of age, and dentin mineral density was significantly higher in Fam20C-Tg mice than in WT mice at 12 weeks of age. In contrast, radicular dentin volume and mineral density were significantly decreased in Fam20C-Tg mice compared to those in WT mice (WT, $n=8$ and Tg, $n=4$ at 2 weeks of age; $n=6$ in each group at 4 and 12 weeks of age; $n=4$ in each group at 24 weeks of age). **d** High-resolution μ CT images at 12 weeks of age. In the coronal dentin of Fam20C-Tg mice, the area with high mineral density (blue) was increased, whereas the area with low dentin density (yellow) was decreased. Each coronal plane (**d1–d3**, **e1–e3**) corresponds to each cut face of the sagittal plane (**d1–d3** in **d**, **e1–e3** in **e**). The indicator showed the density in 255 colors, with higher numbers indicating higher density. *Versus WT mice; * $p < 0.05$; ** $p < 0.01$; *** $p < 0.001$. WT WT mice, Tg Fam20C-Tg mice

argyrophilic tubule structure in either Fam20C-Tg or WT mice (data not shown). Double fluorochrome labeling analyses revealed that the mineral appositional rate in radicular dentin was significantly decreased in Fam20C-Tg compared to WT mice (Fig. 4f).

Odontoblast abnormalities in Fam20C-Tg mice

To examine odontoblast abnormalities in Fam20C-Tg mice, the expression and distribution of DSPP, which is specific to dentin and is its most abundant non-collagen protein, were investigated. Immunohistochemical staining revealed that the immunoreactivities of DSP and DPP were attenuated in the dentin and odontoblasts of Fam20C-Tg mice compared to those of WT mice at 4 weeks of age (Fig. 5a–d). Also, at 12 weeks of age, DPP content was decreased in dentin of Fam20C-Tg mice compared to WT mice (Fig. 3a in Supplementary Material 1). In particular, DSP- and DPP-positive signals were weaker in radicular dentin and odontoblasts than in coronal odontoblasts in Fam20C-Tg mice at 4 and 12 weeks (Fig. 5a–d; Fig. 3a in Supplementary Material 1). Quantitative analysis of DPP in the upper first molars of 4-week-old mice showed a decrease in DPP content in the dentin of Fam20C-Tg mice compared to WT mice (Fig. 5e). This suggests dysfunctional aspects of Fam20C-Tg odontoblasts, including a decrease in DSPP production.

Histological examination of coronal odontoblasts revealed no difference between Fam20C-Tg and WT mice. However, radicular odontoblasts were shorter in Fam20C-Tg mice and their shape was cubic, in contrast with the columnar appearance in WT mice (Fig. 6a). At the apical area of the first molar roots, in particular the distal wall of the mesial root in the first molar (Fig. 4a, b), radicular odontoblasts were flat or had disappeared, and abnormal dentin

with embedded cells and no predentin had formed (Fig. 6b, c). Silver impregnation staining revealed argyrophilic osteocyte canalicular-like structures (Fig. 6b1, c1, arrowheads, inset: higher magnification). In contrast, no embedded cells or argyrophilic canalicular-like structures were observed in the radicular dentin of WT mice. FAM20C immunoreactivity was distributed among all marginal cells and embedded cells in the abnormal dentin, as well as in the abnormal dentin matrix (Fig. 6b2, c2). The abnormal dentin formation was not observed in the incisors of Fam20C-Tg mice (data not shown).

Next, we examined the properties of the abnormal dentin by immunohistochemical staining. WT-dentin was negative for OPN (Fig. 6b3), whereas the abnormal dentin in Fam20C-Tg mice was positive (Fig. 6c3). DMP1 showed very weak staining along the dentin tubule structure in WT mice (Fig. 6b4), and diffusely weak staining in the abnormal dentin of Fam20C-Tg mice (Fig. 6c4). DSP showed positive staining mainly along the dentin tubule structure in WT mice (Fig. 6b5), and was diffusely positive in the abnormal dentin of Fam20C-Tg mice (Fig. 6c5). As OPN immunoreactivity was not originally observed in the dentin but was positive in the bone and cementum (Xie et al. 2014), it was considered that this abnormal dentin had both bone and dentin properties. These characteristics were also observed in the radical dentin of the mesial and distal roots at 12 weeks (Fig. 3a, b in Supplementary Material 1). Furthermore, flat cells in the abnormal dentin of Fam20C-Tg mice were negative for the odontoblast-marker NESTIN (Fig. 7a, b), and positive for the osteogenic-marker RUNX2 (Fig. 7c, d, white arrowheads). In the surrounding dental pulp cells, BMP2 immunoreactivity was enhanced in Fam20C-Tg mice compared to WT mice (Fig. 7e, f).

Gene expression analysis of the upper first molars revealed that the mRNA levels of *Runx2*, *Alp*, *Opn*, *Dmp1*, and *Bmp2* were significantly increased in Fam20C-Tg mice compared to WT mice (Fig. 8). There was no significant difference between the two groups in the mRNA levels of *Osx*, *Coll*, *Dspp*, or *Nestin*. The mRNA level of *Dspp*, a specific odontoblast marker, tended to be decreased in Fam20C-Tg mice compared to WT mice; however, in contrast to the significant decrease in DSPP content shown in Fig. 5, the decrease in mRNA was not significant (Fig. 8). Discrepancies between gene expression levels and protein content are occasionally observed, and may be related to the proteolysis time.

These findings indicated that impairment of odontoblast function and differentiation occurred especially in the radicular dentin of Fam20C-Tg mice.

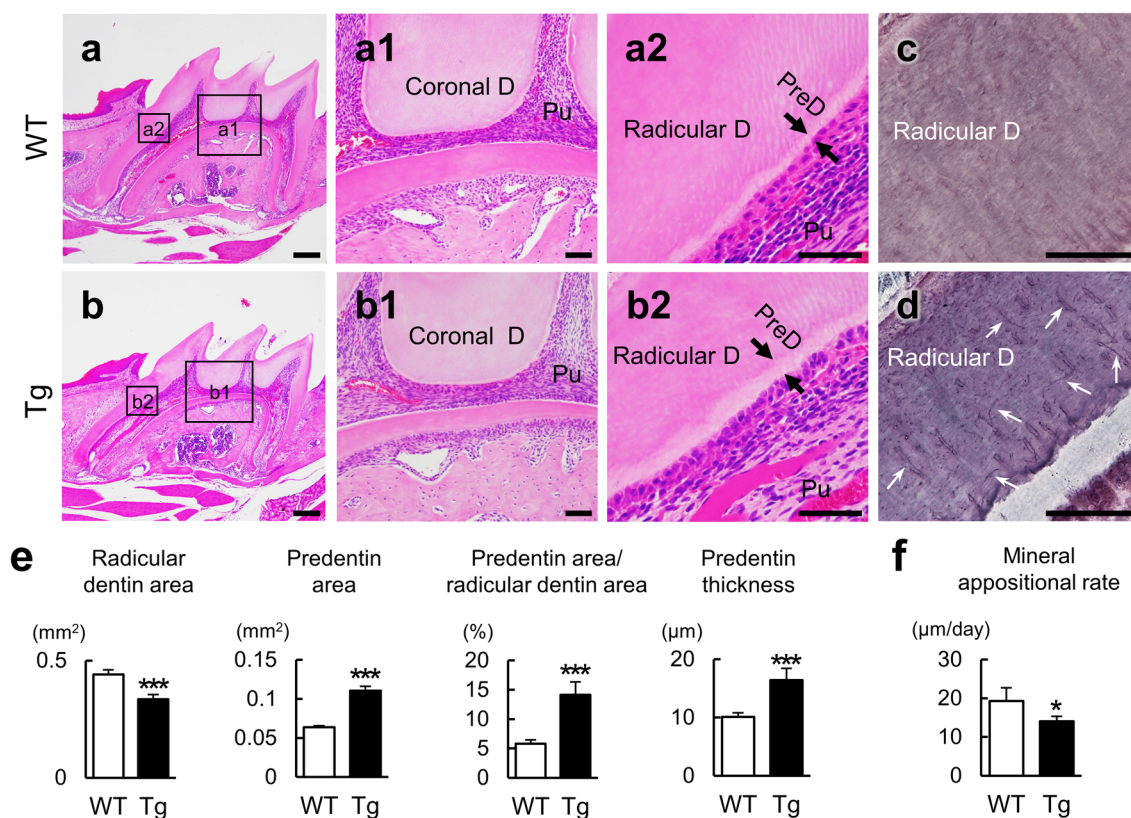


Fig. 4 Histological analysis of coronal and radicular dentin. **a, b** Representative images with hematoxylin and eosin (HE) staining at 4 weeks of age. WT and Fam20C-Tg mice showed no morphological differences in the coronal dentin and pre dentin of upper first molars (**a1, b1**). However, radicular dentin was decreased and the pre dentin width was increased in Fam20C-Tg mice compared to WT mice (**a2, b2** arrows). **c, d** Representative silver impregnation images at 4 weeks of age. In the radicular dentin of Fam20C-Tg mice, argyrophilic dentin tubule structures and canalicular-like structures (white arrowheads) perpendicular to the dentin tubules were observed, whereas these were not evident in WT mice. **e** Morphological meas-

urement of radicular dentin at 4 weeks of age. In upper first molars, the radicular dentin area in Fam20C-Tg mice was significantly reduced compared to that in WT mice. The pre dentin width and area were both significantly increased ($n=6$ in each group). **f** Mineral apposition rate of radicular dentin at 4 weeks of age. Double fluorochrome-labeling analysis of the radicular dentin revealed that dentin mineralization was decreased in Fam20C-Tg mice ($n=6$ in each group). *Versus WT mice; * $p < 0.05$; ** $p < 0.01$; *** $p < 0.001$. WT WT mice, Tg Fam20C-Tg mice, D dentin, Pu pulp. Scale bars 200 μm in **a** and **b** and 50 μm in **a1, a2, b1, b2, c, d**

Abnormal radicular dentin formation in Fam20C-Tg mice

The abnormal dentin in the tooth roots of Fam20C-Tg mice was found in the apex of the upper first molar at 4 weeks of age, i.e., after the start of occlusion, suggesting that occlusal force may have an effect on its formation. To eliminate the effect of occlusal force in root dentin formation, we extracted the mandibular first and second molars, which are opposing teeth, in a non-occluded state. Abnormal dentin formed at the apex of the upper first molar regardless of whether occlusion was present or not (Fig. 4 in Supplementary Material 1). These findings showed that occlusal force did not significantly affect abnormal dentin formation at the apex of the upper first molars of Fam20C-Tg mice.

Next, to investigate the role of Fam20C in root dentin formation without the influence of various environmental factors in vivo, tooth germs were obtained before root formation from 6-day-old WT or Fam20C-Tg mice and were transplanted under the renal capsules of SCID mice. Thirty days after transplantation, tooth germs and the roots that had formed were removed along with the kidneys and were analyzed (Fig. 9a). The developmental stages of 6-day-old WT- and Fam20C-Tg-derived tooth germs were consistent (Fig. 9b). Root-like structures were observed in tooth germs derived from both WT and Fam20C-Tg mice 30 days after transplantation (Fig. 9c), and decreased DPP expression was observed in vivo (Fig. 9c). The root-like structure of tooth germs derived from WT mice exhibited a dentin-like structure containing dentin tubules (Fig. 9d). In contrast,

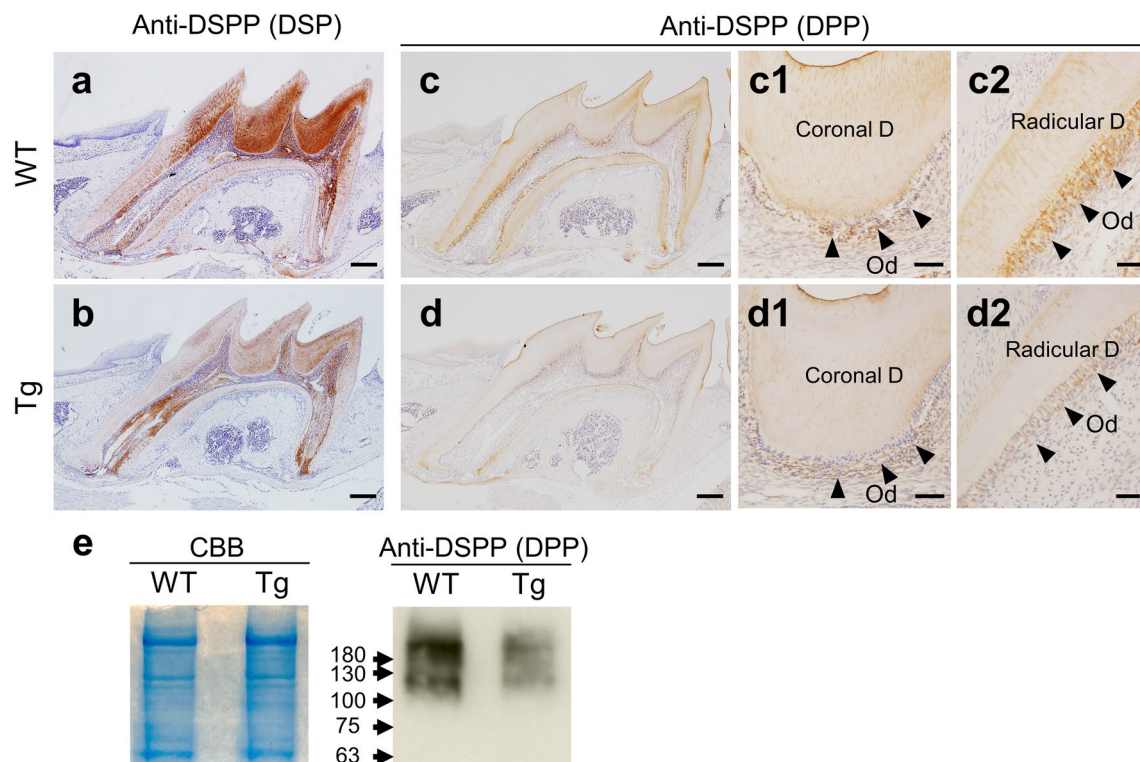


Fig. 5 DSPP expression analysis. **a–d** Representative images of immunohistochemical staining for anti-DSP (**a, b**) and anti-DPP (**c, d**) in WT (**a, c**) and Fam20C-Tg mice (**b, d**) at 4 weeks of age. Immunoreactivities of DSP and DPP were attenuated in the dentin and odontoblasts (arrowheads) of Fam20C-Tg mice compared to those of WT mice. In particular, these signals were weaker in the radicular dentin and odontoblasts than in coronal those in Fam20C-Tg mice

(**c1, d1** coronal dentin, **c2, d2** radicular dentin). **e** Western blotting. CBB staining indicated equal amounts of total proteins extracted from the teeth of WT and Fam20C-Tg mice were subjected. Fam20C-Tg mice produced lower levels of DPP than WT mice. *WT* WT mice, *Tg* Fam20C-Tg mice, *D* dentin, *Od* odontoblast, *CBB* Coomassie brilliant blue. Scale bars 200 μ m in **a–d** and 50 μ m in **c1, c2, d1, d2**

this structure was inconspicuous in the corresponding area of tooth germs derived from Fam20C-Tg mice, and hard tissue with embedded cells had formed, blurring the boundary with the cementum (Fig. 9e). Silver impregnation staining revealed a canalicular-like structure in the radicular dentin-equivalent area of tooth germs derived from Fam20C-Tg mice (Fig. 9d1, e1 inset: higher magnification). The radicular dentin of WT-derived tooth germs was immunopositive for DPP but not for OPN or DMP1 (Fig. 9d2–d4, f). By comparison with WT-one, the hard tissue in the corresponding part of the tooth germ derived from Fam20C-Tg mice showed decreased DPP-, increased DMP1-, and slightly increased OPN-immunoreactivities (Fig. 9e2–e4, f). In addition, RUNX2-positive cells were present in the hard tissue in the corresponding area of tooth germs derived from Fam20C-Tg mice (Fig. 9g, arrowheads).

Thus, in the renal capsule transplantation experiment, there were similar changes to those observed in the abnormal dentin on the apical side of the radicular dentin of Fam20C-Tg mice, confirming that the formation of abnormal dentin was indeed due to the overexpression of Fam20C.

Discussion

Previous studies of Fam20C-deficient mice revealed that inactivation of FAM20C in odontoblasts led to dentin defects as a result of hypophosphatemia and impaired direct roles of FAM20C (Wang et al. 2012, 2015; Liu et al. 2014). However, the direct roles of FAM20C in dentin formation remain unknown. Thus, we examined the roles of FAM20C in dentin formation using Fam20C-Tg mice (Hirose et al. 2020) that overexpressed FAM20C in odontoblasts/osteoblasts and had normal serum phosphate levels. Overexpression of FAM20C increased phosphorylation levels of tooth proteins and phosphorylated broader substrates with other S-x-E/pS motifs, probably including dentin-specific DSPP. In Fam20C-Tg mice, DSPP content was reduced in both coronal and radicular dentin, especially in the latter. Consequently, although the overall phosphorylation level was high in Fam20C-Tg dentin, it was much lower in radicular dentin, possibly due to defects specific to this dentin. Furthermore, on the root apical side, abnormal dentin with bone and dentin properties formed and osteoblast-lineage cells appeared instead of odontoblasts. On the other hand, coronal

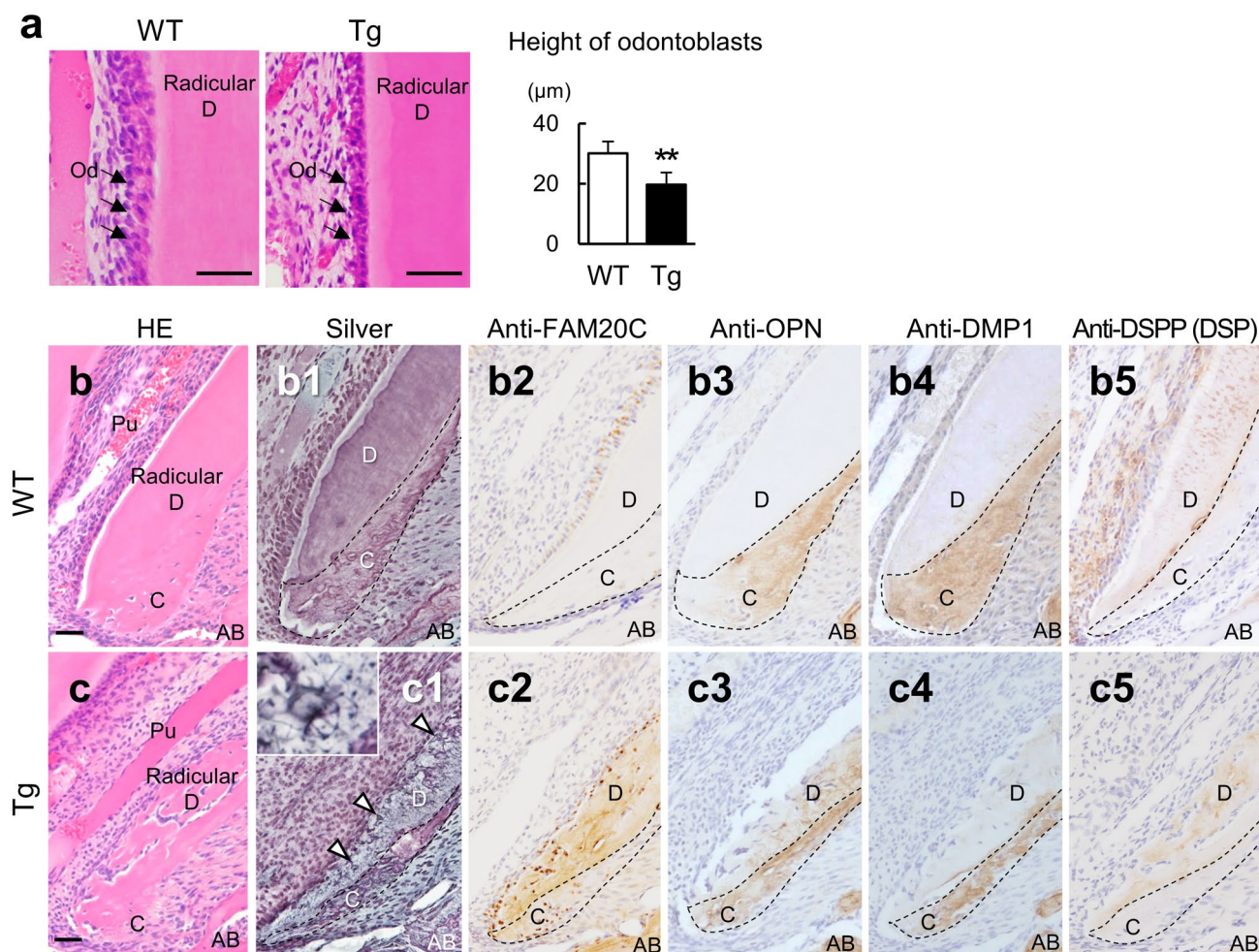


Fig. 6 Analysis of radicular dentin. **a** Representative images of the central part of the radicular dentin (upper first molars at 4 weeks of age) with HE staining. Radicular odontoblasts were shorter in length and have a more cubic shape in Fam20C-Tg compared to WT mice ($n=6$ in each group). **b**, **c** Representative images of the root apex (distal wall of mesial root in upper first molars at 4 weeks of age) with HE, silver impregnation and immunohistochemical staining. HE staining (**b**, **c**), silver impregnation staining (**b1**, **c1**), and immunohistochemical staining for FAM20C (**b2**, **c2**), OPN (**b3**, **c3**), DMP1 (**b4**, **c4**), and DSP (**b5**, **c5**). Abnormal apical-side dentin with embedded

cells and no predentin was seen (**c**), and argyrophilic canalicular-like structures were observed around the embedded cells (**c1** white arrowheads, inset; higher magnification). Abnormal apical-side dentin in Fam20C-Tg mice was positive for FAM20C, OPN, and DSP, and weakly positive for DMP1 (**c2–c5**), whereas normal apical-side dentin in WT mice was negative for OPN (**b3**) *Versus WT mice; ** $p<0.01$, WT WT mice, Tg Fam20C-Tg mice, D dentin, Od odontoblast, Pu pulp, C cementum, AB alveolar bone. Scale bars 50 μm in **a–c**

dentin exhibited reduced volume and an unchanged mineralization level in young mice, but volume recovered and mineralization was normal in mature mice. Thus, coronal and radicular dentin exhibited different amounts of dentin formation and mineralization, possibly due to discrepancies in dentin matrix production and odontoblast differentiation. This study showed that FAM20C-mediated phosphorylation, which is a post-translational modification of odontoblast-derived secreted proteins, is important for dentin formation and mineralization as well as for the regulation of odontoblast function and differentiation.

Comprehensive phosphoproteomic analysis revealed that in Fam20C-Tg mice, but not in WT mice, various secreted proteins had increased phosphorylation levels (Fig. 2a). In Fam20C-Tg mice, the SIBLING proteins OPN, DMP1, and DSP exhibited a larger number of highly phosphorylated residues than in WT mice (Fig. 2b), but some of these residues did not match the S-x-E/pS motif. However, FAM20C reportedly recognizes motifs other than S-x-E/pS (Tagliabracci et al. 2015; Hirose et al. 2020), and therefore FAM20C may phosphorylate more substrates than previously thought. DPP, which is encoded by the same *DSPP* gene as DSP, consists of repeating S-S-D sequences and

is the most highly phosphorylated protein (Prasad et al. 2010). Although DPP has only a few S-x-E/pS motifs, it is also considered to be phosphorylated by FAM20C, as described above, and hence may be more highly phosphorylated in Fam20C-Tg mice. Unfortunately, the comprehensive LC-MS/MS phosphorylation analysis could not be used for DPP. Instead, immunohistochemical analysis revealed that the immunoreactivity of phosphorylated serine was increased in the coronal dentin of Fam20C-Tg mice compared with WT mice (Fig. 2e). DPP is the most abundant non-collagen protein in dentin, and is highly phosphorylated at its serine residues (Prasad et al. 2010). Therefore, the strong immunoreactivity of phosphoserine represents highly phosphorylated DPP in the coronal dentin of Fam20C-Tg mice. GO analysis of the phosphoproteomic results revealed that the secreted proteins that exhibited enhanced phosphorylation in Fam20C-Tg mice are involved in biological functions related to bone formation, hard tissue development, and osteoblast differentiation (Supplementary Material 3). On the molecular function level, they are involved in the binding of calcium ions, growth factors, and extracellular matrix components, and many are thought to contribute to the changes in dentin and odontoblasts observed in Fam20C-Tg mice.

There were no significant changes in coronal dentin mass and morphology in mature Fam20C-Tg mice (at 12 and 24 weeks), but the dentin mass was significantly decreased in the root, where morphological changes were observed. The radicular dentin of Fam20C-Tg mice was characterized by an increased predentin width, lower mineralization rate, and shorter odontoblast length, and silver impregnation staining revealed an argyrophilic dentin tubule structure that was not observed in WT mice. At the root apex, the dentin tubule structures were not apparent and abnormal dentin with embedded cells was present (Fig. 6). Silver argyrophilic staining revealed a canalicular-like structure around the embedded cells. This abnormal dentin immunostained for OPN, which is normally negative in dentin and strongly positive in bone and cementum (Xie et al. 2014). Dentin-specific DSPP also stained positively for the abnormal dentin. In addition, NESTIN-negative, RUNX2-positive cells belonged to the osteoblast lineage (Komori 2020), appeared to be in contact with the abnormal dentin (Fig. 7). Thus, this abnormal dentin seemed to have both bone- and dentin-like characteristics.

Gene expression analysis of the first molars of Fam20C-Tg mice showed significant increases in mRNA expression of *Runx2* and *Opn*, indicating osteoblastic differentiation (Fig. 8). Although no significant difference was observed in the mRNA expression of *Dspp* and *Nestin*, both of which are markers of odontoblast differentiation, protein analyses revealed that the DSPP content in both the coronal and radicular dentin was significantly decreased and that NESTIN

expression was reduced in radicular but not coronal dentin. No apparent morphological changes were observed in the coronal dentin of Fam20C-Tg mice. However, the decreased DSPP content and increased mineral density of coronal dentin in mature mice indicated that Fam20C overexpression affected the coronal dentin. Therefore, although the effect on coronal and radicular dentin differs in degree, Fam20C overexpression appeared to cause changes in both.

The decrease in production of DSPP, which is important for dentin formation and mineralization (Prasad et al. 2010; Suzuki et al. 2012), likely greatly influenced dentin formation in Fam20C-Tg mice. The DSPP content in radicular dentin is approximately half of that in coronal dentin (Takagi et al. 1988), and further reduction in DSPP in Fam20C-Tg mice may have significantly contributed to the hypoplasia of radicular dentin in these mice. Regarding the amount of DSPP necessary for dentin formation, a rescue experiment in which DSPP was expressed at various levels in DSPP-deficient mice revealed that DSPP at a level 25% of that in WT mice was required for dentin formation; with 5% DSPP content, only partial dentin recovery was observed (Lim et al. 2021). While the DSPP content decreased throughout the dentin in Fam20C-Tg mice, DSPP immunoreactivity in the coronal dentin persisted (Fig. 5a–d). Furthermore, the phosphoserine immunoreactivity in the coronal dentin of Fam20C-Tg mice was stronger than that in WT mice (Fig. 2c–e), suggesting enhanced phosphorylation of residual DSPP. If the coronal dentin in Fam20C-Tg mice had more than 25% of the amount of residual DSPP content in WT mice, the amount of residual DSPP would have been enhanced in mineralization of the coronal dentin. This may have caused an increase in the coronal dentin. In contrast, in the radicular dentin of Fam20C-Tg mice, especially in the apex, DSPP immunoreactivity was attenuated compared to that in WT mice (Fig. 5a–d), and the immunoreactivity of phosphorylated serine was nearly eliminated (Fig. 2c–e). Therefore, there was an insufficient amount of DSPP, which reduced the phosphorylation level and led to the formation of abnormal dentin at the root apex.

The radicular odontoblasts of Fam20C-Tg mice showed morphological abnormalities (Fig. 6a–c). Renal subcapsular transplantation of teeth germs to eliminate the influence of environmental factors, also replicated apical abnormal dentin of Fam20C-Tg mice (Fig. 9b–e), corroborating that FAM20C overexpression indeed caused the abnormal dentin. In addition, the abnormal dentin had both bone- and dentin-like matrix, and some RUNX2-positive cells appeared on the abnormal dentin, implying that the radicular odontoblasts exhibited abnormal differentiation by FAM20C overexpression. RUNX2 is a master transcription factor of osteoblast lineage differentiation; it determines the direction of differentiation from mesenchymal cells to osteoblast

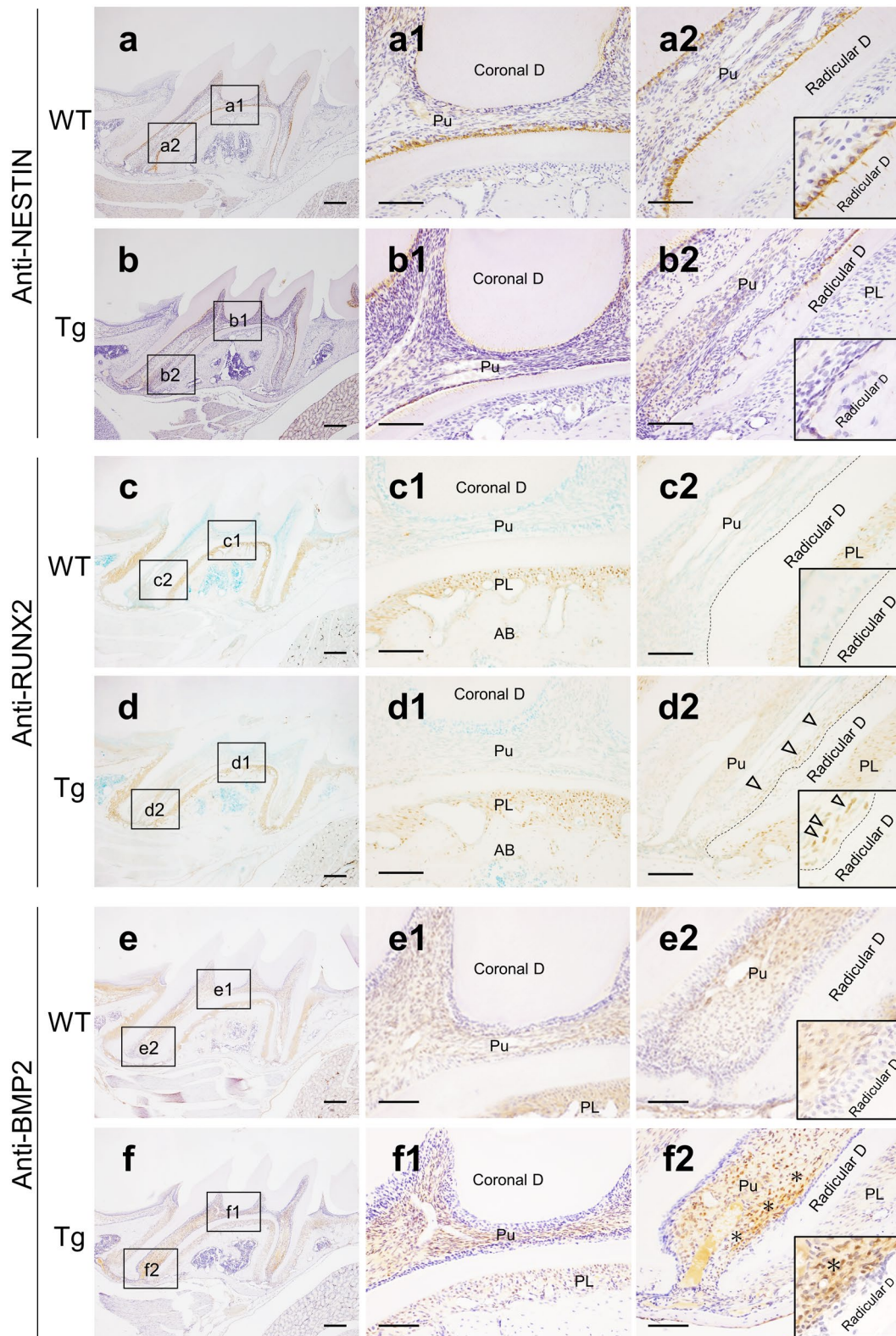


Fig. 7 Analysis of odontoblast differentiation. **a–f** Representative images of upper first molar of WT (**a, c, e**) and Fam20C-Tg mice (**b, d, f**) at 4 weeks of age with immunohistochemical staining for NESTIN (**a, b**), RUNX2 (**c, d**) and BMP2 (**e, f**). **a, b** NESTIN-immunoreactivity was not observed in the surface cells (odontoblasts) on the apical area of radicular dentin of Fam20C-Tg mice (**b2**), whereas its immunoreactivity was detected in all the other odontoblasts of both WT (**a1**) and Fam20C-Tg mice (**b1**). **c, d** RUNX2-immunoreactivity was observed in the surface cells (odontoblasts) on the apical area of radicular dentin of Fam20C-Tg mice (**d2**), whereas its immunoreactivity was not detected in all the other odontoblasts of both WT (**c1**) and Fam20C-Tg mice (**d1**). **e, f** BMP2 immunoreactivity in dental pulp cells, especially around the RUNX2-positive cells, was enhanced in Fam20C-Tg mice (**f, f2** asterisks) compared to WT mice (**e**). Each solid frame indicated higher magnifications of figures **a2, b2, c2, d2, e2** and **f2**, respectively. *WT* WT mice, *Tg* Fam20C-Tg mice, *D* dentin, *AB* alveolar bone, *Pu* pulp, *PL* periodontal ligament. *Scale bars* 250 μ m in **a–f**; 100 μ m in **a1, a2, b1, b2, c1, c2, d1, d2, e1, e2, f1, f2**

lineage cells and regulates numerous bone- and dentin-related genes (Komori 2010, 2020). In the dentin, RUNX2 is expressed in the early stage of odontoblast differentiation, but its expression decreases in the subsequent differentiation and maturation stages (Komori 2010). In a study of mice overexpressing RUNX2 in odontoblasts, abnormal dentin similar to repaired dentin was observed, accompanied by cell inclusions and the disappearance of dentin tubules (Miyazaki et al. 2008). That study also demonstrated argyrophilic canalicular-like structures in the crown and root. The abnormal dentin showed decreased DSPP and increased OPN expressions and had spindle-shaped odontoblasts that overexpressed RUNX2. This phenomenon is similar to that observed in the root apex in Fam20C-Tg mice in the present study. Based on the above, the abnormal dentin in the apex of the radicular dentin in Fam20C-Tg mice likely represented a change caused by RUNX2 expression in odontoblasts. During dentin repair, OPN and DMP1 expression increases, and since Runx2-positive cells are involved in this process (Zhao et al. 2007), Fam20C expression may increase upstream of RUNX2 expression. The abnormal shortening of the root odontoblasts seemed also to be due to RUNX2 expression in these odontoblasts at very low levels that could not be detected by immunohistochemistry. The increased mRNA levels of *Runx2*, *Alp*, *Opn*, *Dmp1*, and *Bmp2* in the first molars may indicate abnormal differentiation of root odontoblasts into osteoblast lineage cells. The mechanism by which FAM20C overexpression in odontoblasts regulates RUNX2 expression remains unclear. However, in the upper first molars of Fam20C-Tg mice, increased *Bmp2* mRNA expression (Fig. 8) and increased BMP2 immunoreactivity were observed on the pulp side of RUNX2-positive root odontoblasts (Fig. 7). This indicates that BMP2 can regulate RUNX2 expression. BMP signals are important for bone and

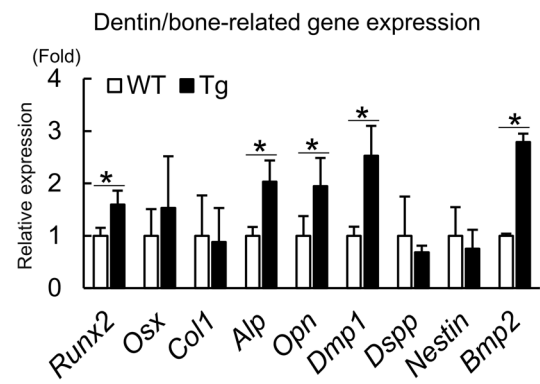


Fig. 8 Gene expression analysis. In upper first molars of 4-week-old Fam20C-Tg mice, mRNA levels of *Runx2*, *Alp*, *Opn*, *Dmp1*, and *Bmp2* were significantly increased compared to WT mice. mRNA levels of *Dspp* and *Nestin*, which are odontoblast markers, were decreased, albeit not significantly. *Versus WT mice; * $p < 0.05$. *WT* WT mice, *Tg* Fam20C-Tg mice

dentin development, as well as for osteoblast and odontoblast differentiation. BMP signaling has been shown to be suppressed in Fam20C-deficient osteoblast/pulp mesenchymal cell lines (Liu et al. 2018a, b). Therefore, overexpression of FAM20C may induce RUNX2 expression in odontoblasts by enhancing the BMP signal.

During tooth development in normal mice, FAM20C is expressed in dental papilla cells that are in contact with the enamel epithelium in the late cap-to-bell-shape stages. In differentiated odontoblasts, its expression increases. However, after 3 weeks of age, FAM20C expression has been shown to decrease with aging, and it almost disappears at 7 weeks of age (Wang et al. 2010). Little information is available regarding the role of FAM20C during early differentiation into odontoblasts. However, in vitro experiments using dental pulp stem cells with Fam20C knock-out or knock-down have shown reduced expression of odontoblast markers (*Dmp1* and *Dspp* mRNA) and suppressed formation of calcification nodules (Hao et al. 2007; Li et al. 2018; Liu et al. 2018b). Thus, FAM20C is important during the early differentiation of dental pulp stem cells into odontoblasts. In Fam20C-Tg mice, which overexpressed FAM20C in synchrony with type I collagen expression, the FAM20C overexpression occurred in the secretory and mature odontoblast stages, after the differentiation into odontoblasts. In normal development, during the differentiation of dental papilla cells to pre-odontoblasts, the latter have been shown to express RUNX2, which disappears when they further differentiate into odontoblasts (Komori 2010). Constitutive overexpression of FAM20C therefore appeared to interfere with odontoblast function and maturation during late differentiation.

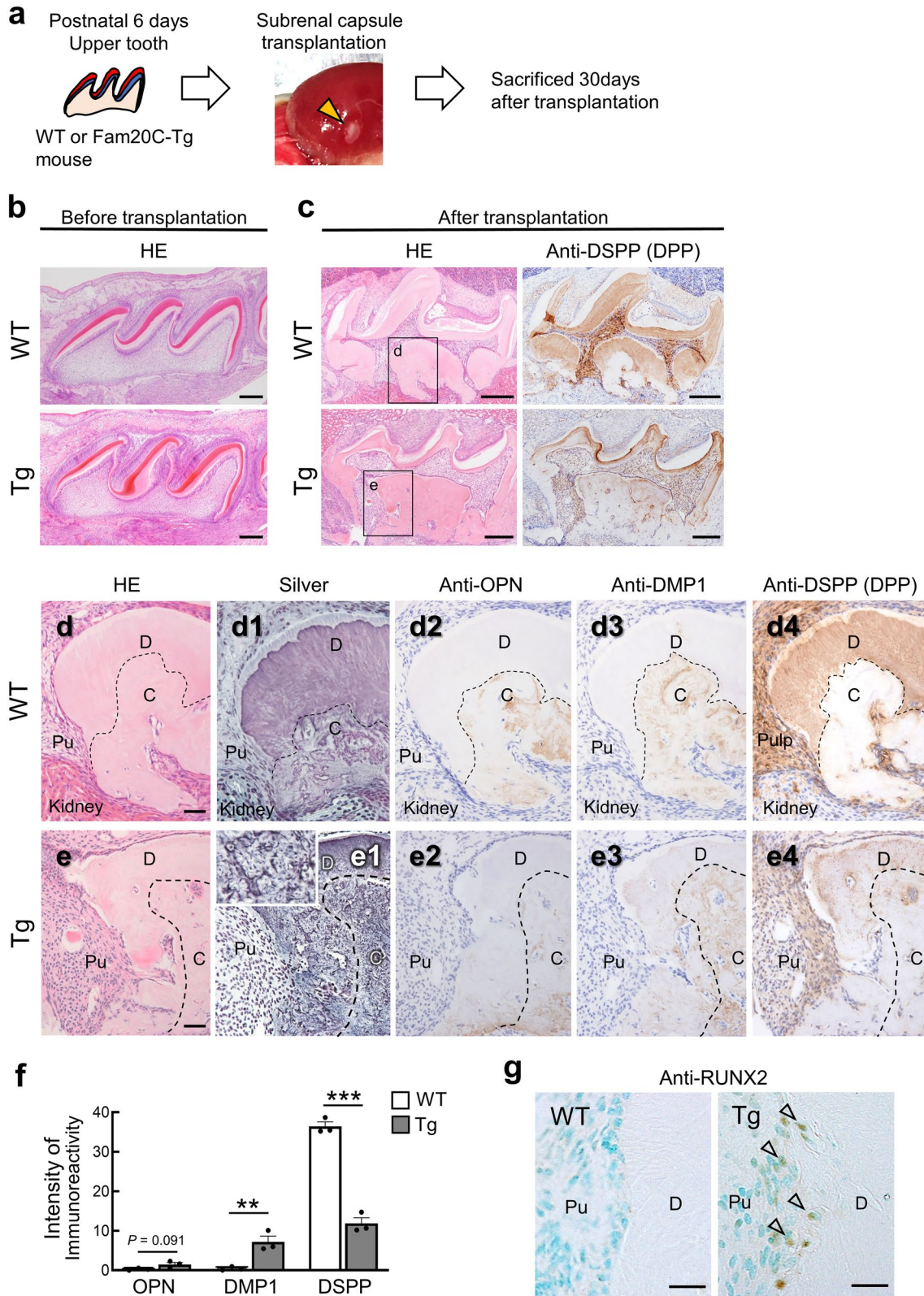


Fig. 9 Renal subcapsular transplantation experiment of tooth germs. **a** Experimental procedure. Yellow arrowhead indicated transplanted tooth germ. **b** Six-day-old tooth germ at the time of transplantation. The developmental stages of WT- and Fam20C-Tg-derived tooth germs were consistent, and root formation was not yet observed. **c** Representative images of tooth germ at 30 days after transplantation with HE and immunohistochemical staining. A dental root-like structure was observed in both WT ($n=5$) and Fam20C-Tg tooth germs ($n=3$), and DPP expression was decreased in Fam20C-Tg tooth germs, as observed in the teeth of Fam20C-Tg mice. **d, e** Representative images of root equivalent of the tooth germ with HE, silver impregnation and immunohistochemical staining. **d** and **e** Higher magnifications of the solid black frames in WT and Fam20C-Tg mice in **c**, respectively. HE staining (**d, e**), silver impregnation staining (**d1, e1**), and immunohistochemical staining for OPN (**d2, e2**), DMP1 (**d3, e3**), and DPP (**d4, e4**). In the Fam20C-Tg-derived tooth germ corresponding to the root, the dentin tubule structure was inconspicuous, and hard tissue with embedded cells had formed. Canalicular-like structures were observed in the part corresponding to the root dentin. The radicular dentin of WT-derived tooth germ was positive for DPP but almost negative for OPN or DMP1. In contrast, the corresponding area of tooth germs derived from Fam20C-Tg mice was weakly positive for DMP1, light positive for DPP, and very slightly positive for OPN (**e2–e4**). **f** Quantification of OPN, DMP1, DPP immunoreactivity in the root equivalent of the tooth germ. The points indicate immunoreactivity values of OPN, DMP1, DPP ($n=3$ in each group). **g** Representative images of surface cells on root equivalent with immunohistochemical staining. Some RUNX2-positive cells were observed on the part corresponding to the Fam20C-Tg root (white arrowheads). *Versus WT mice; ** $p < 0.01$; *** $p < 0.001$. WT WT mice, Tg Fam20C-Tg mice, D dentin equivalent, C cementum equivalent, Pu pulp. Scale bars: 200 μm in **b** and **c** and 50 μm in **d** and **e** 25 μm in **g**

Supplementary Information The online version contains supplementary material available at <https://doi.org/10.1007/s10735-023-10123-y>.

Acknowledgements The phosphoproteomic analysis was performed by Medical ProteoScope (Yokohama, Japan), and the authors would like to acknowledge the support of the staff there.

Author contributions All authors contributed to this work, and reviewed and approved the manuscript for submission. KN and KH contributed equally to this work. KN: Investigation, Data Curation, Visualization. KH: Methodology, Validation, Investigation, Resources, Data Curation, Writing—Original Draft, Writing—Review and Editing, Visualization, Supervision, Project Administration, Funding Acquisition. YU: Resources. KH: Investigation, Resources, Supervision. RA: Investigation, Visualization. NU: Supervision. TK: Methodology, Supervision. ST: Conceptualization, Methodology, Validation, Resources, Data Curation, Writing—Original Draft, Writing—Review and Editing, Visualization, Supervision, Project Administration, Funding Acquisition.

Funding This work was supported by Japan Society for the Promotion of Science (JSPS) KAKENHI Grant Numbers JP17H04368, JP26670801, JP19K18944, and JP21K16930.

Data availability The data used to support the findings of this study are available from the corresponding author upon request.

Declarations

Conflict of interest All the authors have no relevant financial or non-financial interests to disclose.

Ethical approval All animal experiments were reviewed and approved by the Intramural Animal Use and Care Committee of Osaka University Graduate School of Dentistry (Permit Number R-01-006-0).

References


- Acevedo AC, Poulter JA, Alves PG, de Lima CL, Castro LC, Yamaguti PM, Paula LM, Parry DA, Logan CV, Smith CE, Johnson CA, Inglehearn CF, Mighell AJ (2015) Variability of systemic and orodental phenotype in two families with non-lethal Raine syndrome with FAM20C mutations. *BMC Med Genet* 16:8
- Al-Hashimi N, Lafont AG, Delgado S, Kawasaki K, Sire JY (2010) The enamel genes in lizard, crocodile, and frog and the pseudogene in the chicken provide new insights on enamel evolution in tetrapods. *Mol Biol Evol* 27:2078–2094
- Butler WT, Bhowm M, DiMuzio MT, Cothran WC, Linde A (1983) Multiple forms of rat dentin phosphoproteins. *Arch Biochem Biophys* 225:178–186
- Delsuc F, Gasse B, Sire JY (2015) Evolutionary analysis of selective constraints identifies ameloblastin (AMBN) as a potential candidate for amelogenesis imperfecta. *BMC Evol Biol* 15:148
- Deshpande AS, Fang PA, Zhang X, Jayaraman T, Sfeir C, Beniash E (2011) Primary structure and phosphorylation of dentin matrix protein 1 (DMP1) and dentin phosphophoryn (DPP) uniquely determine their role in biomineralization. *Biomacromolecules* 12:2933–2945
- Faundes V, Castillo-Taucher S, Gonzalez-Hormazabal P, Chandler K, Crosby A, Chioza B (2014) Raine syndrome: an overview. *Eur J Med Genet* 57:536–542
- Feng JQ, Luan X, Wallace J, Jing D, Ohshima T, Kulkarni AB, D'Souza RN, Kozak CA, MacDougall M (1998) Genomic organization, chromosomal mapping, and promoter analysis of the mouse dentin sialophosphoprotein (dspp) gene, which codes for both dentin sialoprotein and dentin phosphoprotein. *J Biol Chem* 273:9457–9464
- George A, Veis A (2008) Phosphorylated proteins and control over apatite nucleation, crystal growth, and inhibition. *Chem Rev* 108:4670–4693
- Hao J, Narayanan K, Muni T, Ramachandran A, George A (2007) Dentin matrix protein 4, a novel secretory calcium-binding protein that modulates odontoblast differentiation. *J Biol Chem* 282:15357–15365
- Hirose K, Ishimoto T, Usami Y, Sato S, Oya K, Nakano T, Komori T, Toyosawa S (2020) Overexpression of Fam20C in osteoblast in vivo leads to increased cortical bone formation and osteoclastic bone resorption. *Bone* 138:115414
- Ishikawa HO, Xu A, Ogura E, Manning G, Irvine KD (2012) The Raine syndrome protein FAM20C is a Golgi kinase that phosphorylates bio-mineralization proteins. *PLoS ONE* 7:e42988
- Komori T (2010) Regulation of bone development and extracellular matrix protein genes by RUNX2. *Cell Tissue Res* 339:189–195
- Komori T (2020) Molecular mechanism of Runx2-dependent bone development. *Mol Cells* 43:168–175
- Kusuzaki K, Kageyama N, Shinjo H, Takeshita H, Murata H, Hashiguchi S, Ashihara T, Hirasawa Y (2000) Development of bone canaliculi during bone repair. *Bone* 27:655–659

- Li Q, Yi B, Feng Z, Meng R, Tian C, Xu Q (2018) FAM20C could be targeted by TET1 to promote odontoblastic differentiation potential of human dental pulp cells. *Cell Prolif* 51:e12426
- Lim D, Wu KC, Lee A, Saunders TL, Ritchie HH (2021) DSPP dosage affects tooth development and dentin mineralization. *PLoS ONE* 16:e0250429
- Liu P, Zhang H, Liu C, Wang X, Chen L, Qin C (2014) Inactivation of Fam20C in cells expressing type I collagen causes periodontal disease in mice. *PLoS One* 9:e114396
- Liu P, Ma S, Zhang H, Liu C, Lu Y, Chen L, Qin C (2017) Specific ablation of mouse Fam20C in cells expressing type I collagen leads to skeletal defects and hypophosphatemia. *Sci Rep* 7:3590
- Liu C, Zhang H, Jani P, Wang X, Lu Y, Li N, Xiao J, Qin C (2018a) FAM20C regulates osteoblast behaviors and intracellular signaling pathways in a cell-autonomous manner. *J Cell Physiol* 233:3476–3486
- Liu C, Zhou N, Wang Y, Zhang H, Jani P, Wang X, Lu Y, Li N, Xiao J, Qin C (2018b) Abrogation of Fam20c altered cell behaviors and BMP signaling of immortalized dental mesenchymal cells. *Exp Cell Res* 363:188–195
- Liu J, Saiyin W, Xie X, Mao L, Li L (2020) Ablation of Fam20c causes amelogenesis imperfecta via inhibiting smad dependent BMP signaling pathway. *Biol Direct* 15:16
- Miyazaki T, Kanatani N, Rokutanda S, Yoshida C, Toyosawa S, Nakamura R, Takada S, Komori T (2008) Inhibition of the terminal differentiation of odontoblasts and their transdifferentiation into osteoblasts in Runx2 transgenic mice. *Arch Histol Cytol* 71:131–146
- Nagata K, Kawakami T, Kurata Y, Kimura Y, Suzuki Y, Nagata T, Sakuma Y, Miyagi Y, Hirano H (2015) Augmentation of multiple protein kinase activities associated with secondary imatinib resistance in gastrointestinal stromal tumors as revealed by quantitative phosphoproteome analysis. *J Proteomics* 115:132–142
- Oya K, Ishida K, Nishida T, Sato S, Kishino M, Hirose K, Ogawa Y, Ikebe K, Takeshige F, Yasuda H, Komori T, Toyosawa S (2017) Immunohistochemical analysis of dentin matrix protein 1 (Dmp1) phosphorylation by Fam20C in bone: implications for the induction of biomineralization. *Histochem Cell Biol* 147:341–351
- Prasad M, Butler WT, Qin C (2010) Dentin sialophosphoprotein in biomineralization. *Connect Tissue Res* 51:404–417
- Qin C, Baba O, Butler WT (2004) Post-translational modifications of sibling proteins and their roles in osteogenesis and dentinogenesis. *Crit Rev Oral Biol Med* 15:126–136
- Raine J, Winter RM, Davey A, Tucker SM (1989) Unknown syndrome: microcephaly, hypoplastic nose, exophthalmos, gum hyperplasia, cleft palate, low set ears, and osteosclerosis. *J Med Genet* 26:786–788
- Roach PJ (1991) Multisite and hierarchal protein phosphorylation. *J Biol Chem* 266:14139–14142
- Simpson MA, Hsu R, Keir LS, Hao J, Sivapalan G, Ernst LM, Zackai EH, Al-Gazali LI, Hulskamp G, Kingston HM, Prescott TE, Ion A, Patton MA, Murday V, George A, Crosby AH (2007) Mutations in FAM20C are associated with lethal osteosclerotic bone dysplasia (Raine syndrome), highlighting a crucial molecule in bone development. *Am J Hum Genet* 81:906–912
- Sreenath T, Thyagarajan T, Hall B, Longenecker G, D'Souza R, Hong S, Wright JT, MacDougall M, Sauk J, Kulkarni AB (2003) Dentin sialophosphoprotein knockout mouse teeth display widened predentin zone and develop defective dentin mineralization similar to human dentinogenesis imperfecta type III. *J Biol Chem* 278:24874–24880
- Suzuki S, Haruyama N, Nishimura F, Kulkarni AB (2012) Dentin sialophosphoprotein and dentin matrix protein-1: two highly phosphorylated proteins in mineralized tissues. *Arch Oral Biol* 57:1165–1175
- Tagliabracci VS, Engel JL, Wen J, Wiley SE, Worby CA, Kinch LN, Xiao J, Grishin NV, Dixon JE (2012) Secreted kinase phosphorylates extracellular proteins that regulate biomineralization. *Science* 336:1150–1153
- Tagliabracci VS, Pinna LA, Dixon JE (2013) Secreted protein kinases. *Trends Biochem Sci* 38:121–130
- Tagliabracci VS, Wiley SE, Guo X, Kinch LN, Durrant E, Wen J, Xiao J, Cui J, Nguyen KB, Engel JL, Coon JJ, Grishin N, Pinna LA, Pagliarini DJ, Dixon JE (2015) A single kinase generates the majority of the secreted phosphoproteome. *Cell* 161:1619–1632
- Takagi Y, Nagai H, Sasaki S (1988) Difference in noncollagenous matrix composition between crown and root dentin of bovine incisor. *Calcif Tissue Int* 42:97–103
- Toyosawa S, Shintani S, Fujiwara T, Ooshima T, Sato A, Ijuhin N, Komori T (2001) Dentin matrix protein 1 is predominantly expressed in chicken and rat osteocytes but not in osteoblasts. *J Bone Miner Res* 16:2017–2026
- Vogel P, Hansen GM, Read RW, Vance RB, Thiel M, Liu J, Wronski TJ, Smith DD, Jeter-Jones S, Brommage R (2012) Amelogenesis imperfecta and other biomineralization defects in Fam20a and Fam20c null mice. *Vet Pathol* 49:998–1017
- Wang X, Hao J, Xie Y, Sun Y, Hernandez B, Yamoah AK, Prasad M, Zhu Q, Feng JQ, Qin C (2010) Expression of FAM20C in the osteogenesis and odontogenesis of mouse. *J Histochem Cytochem* 58:957–967
- Wang X, Wang S, Lu Y, Gibson MP, Liu Y, Yuan B, Feng JQ, Qin C (2012) FAM20C plays an essential role in the formation of murine teeth. *J Biol Chem* 287:35934–35942
- Wang X, Jung J, Liu Y, Yuan B, Lu Y, Feng JQ, Qin C (2013) The specific role of FAM20C in amelogenesis. *J Dent Res* 92:995–999
- Wang X, Wang J, Liu Y, Yuan B, Ruest LB, Feng JQ, Qin C (2015) The specific role of FAM20C in dentinogenesis. *J Dent Res* 94:330–336
- Xie X, Ma S, Li C, Liu P, Wang H, Chen L, Qin C (2014) Expression of small integrin-binding LIgand N-linked glycoproteins (SIBLINGs) in the reparative dentin of rat molars. *Dent Traumatol* 30:285–295
- Zhang X, Zhao J, Li C, Gao S, Qiu C, Liu P, Wu G, Qiang B, Lo WH, Shen Y (2001) DSPP mutation in dentinogenesis imperfecta Shields type II. *Nat Genet* 27:151–152
- Zhang H, Xie X, Liu P, Liang T, Lu Y, Qin C (2018) Transgenic expression of dentin phosphoprotein (DPP) partially rescued the dentin defects of DSPP-null mice. *PLoS ONE* 13:e0195854
- Zhang H, Li L, Kesterke MJ, Lu Y, Qin C (2019) High-phosphate Diet improved the skeletal development of Fam20c-Deficient mice. *Cells Tissues Organs* 208:25–36
- Zhang H, Xu Q, Lu Y, Qin C (2021) Effect of high phosphate diet on the formation of dentin in Fam20c-deficient mice. *Eur J Oral Sci* 129:e12795
- Zhao C, Hosoya A, Kurita H, Hu T, Hiraga T, Ninomiya T, Yoshida K, Yoshida N, Takahashi M, Kurashina K, Ozawa H, Nakamura H (2007) Immunohistochemical study of hard tissue formation in the rat pulp cavity after tooth replantation. *Arch Oral Biol* 52:945–953

Publisher's Note Springer Nature remains neutral with regard to jurisdictional claims in published maps and institutional affiliations.

Springer Nature or its licensor (e.g. a society or other partner) holds exclusive rights to this article under a publishing agreement with the author(s) or other rightsholder(s); author self-archiving of the accepted manuscript version of this article is solely governed by the terms of such publishing agreement and applicable law.

Authors and Affiliations

Kohei Naniwa^{1,2} · Katsutoshi Hirose¹  · Yu Usami¹ · Kenji Hata³ · Rikita Araki⁴ · Narikazu Uzawa² · Toshihisa Komori⁵ · Satoru Toyosawa¹

✉ Satoru Toyosawa
toyosawa.satoru.dent@osaka-u.ac.jp
Kohei Naniwa
k-naniwa@dent.osaka-u.ac.jp
Katsutoshi Hirose
hirose.katsutoshi.dent@osaka-u.ac.jp
Yu Usami
usami.yuu.dent@osaka-u.ac.jp
Kenji Hata
hata.kenji.dent@osaka-u.ac.jp
Rikita Araki
rikita.araki@bruker.com
Narikazu Uzawa
uzawa.narikazu.dent@osaka-u.ac.jp
Toshihisa Komori
komorit@nagasaki-u.ac.jp

- ¹ Department of Oral and Maxillofacial Pathology, Osaka University Graduate School of Dentistry, 1-8 Yamadaoka, Suita, Osaka 565-0871, Japan
- ² Department of Oral & Maxillofacial Oncology and Surgery, Osaka University Graduate School of Dentistry, 1-8 Yamadaoka, Suita, Osaka 565-0871, Japan
- ³ Department of Molecular and Cellular Biochemistry, Osaka University Graduate School of Dentistry, 1-8 Yamadaoka, Suita, Osaka 565-0871, Japan
- ⁴ Bruker Japan K.K. BioSpin Division, Application Department, 3-9 Kanagawaku Moriyacho, Yokohama, Kanagawa 221-0022, Japan
- ⁵ Department of Molecular Bone Biology, Nagasaki University Graduate School of Biomedical Sciences, 1-7-1 Sakamoto, Nagasaki 852–8588, Japan